LOKIBASE: THE DEVICE FOR SEISMIC ISOLATION OF PALLET RACKING SYSTEMS

LOKIBASE: DISPOSITIVO PER L'ISOLAMENTO SISMICO DI SCAFFALATURE METALLICHE PORTAPALLET (Seconda parte)

Ing. Marco Ferrari*

6 SIMPIFIED SHAPE OPTIMIZATION ANALYSES OF THE LOKIBASE CYLINDRICAL BEAM DAMPER

6.1 Introduction

This chapter gives shape optimization analyses of the LOKIBASE cylindrical beam damper for a further reduction in the horizontal force F value.

Section 6.2 gives a simplified theoretical analysis of the LOKIBASE cylindrical beam damper with conical segment at the top for zero and non-zero friction. For the maximum displacement d_2, a comparison of the horizontal forces at the top of the cylindrical beam damper with conical segment (F^*_2 in the Figure 6.1) and at the top of the cylindrical beam damper (F_2 in the Figure 3.1) is made.

Section 6.4 gives a simplified theoretical analysis of the LOKIBASE cylindrical beam damper with double-circular cross section at the bottom (in the plastic hinge segment). For the maximum displacement d_2 and two LOKI devices with a k value of 6 N/mm, a comparison of the horizontal force acting in Z-direction (down-aisle direction, the weakest) on the LOKIBASE device with optimized cylindrical beam damper ($F^{dc}_{2,Z,LOKIBASE}$ in the Table 6.7.2) and the horizontal force acting in the same direction on the LOKIBASE device with cylindrical beam damper ($F^{c}_{2,LOKIBASE}$ in the Table 6.6) is made.

6.2 Optimization analysis of the LOKIBASE cylindrical beam damper. Conical segment at the top and zero and non-zero friction. This section shows how the value of the horizontal force F decrease under large displacements when the friction between the segment at the top of the cylindrical beam damper and the device (horizontal plate welded to the horizontal strut at the bottom of the upright frame) which engages it is zero and non-zero and when the shape of the cylindrical beam damper in the engaged length is conical. The horizontal force F can act at a fixed height because sliding is possible between the cylindrical beam damper and the hole in the horizontal plate.

Figure 6.1 shows the main dimensions for the maximum displacement d_2 (Limit state for collapse prevention, SLC) at the top.

For a zero value of the angle of rotation α of the plastic hinge at the bottom of the cantilever, the mathematical relation between the force perpendicular to the surface of the conical segment of the cylindrical beam damper $F^*_{1,perp}$ and M_{pl} is given by:

$$F^*_{1,perp} * H^*_{1,N} + F^*_{1,paral} * H^*_{1,V} = M_{pl} \text{ where } F^*_{1,paral} = \mu * F^*_{1,perp} \quad [6.1]$$

$$M_{pl} = F^*_{1,perp} * (H^*_{1,N} + \mu * H^*_{1,V}) \quad [6.2]$$

For a non-zero value of the angle of rotation of the plastic hinge at the bottom of the cantilever, the mathematical relation between the force perpendicular to the surface of the conical segment of the cylindrical beam damper $F^*_{2,perp}$ and M_{pl} is given by:

$$F^*_{2,perp} * H^*_{2,N} + F^*_{2,paral} * H^*_{2,V} = M_{pl} \text{ where } F^*_{2,paral} = \mu * F^*_{2,perp} \quad [6.3]$$

$$F^*_{2,perp} * (H^*_{2,N} + \mu * H^*_{2,V}) = M_{pl} \quad [6.4]$$

$$F^*_{2,perp} = \frac{M_{pl}}{(H^*_{2,N} + \mu * H^*_{2,V})} \quad [6.5]$$

[1] La prima parte è stata pubblicata sul numero 3/2019 della rivista

* Corresponding author. E-mail address: marco.ferrari@tin.it

In view of eqn. [6.2], equation [6.5] can be written as:

$$F^*_{2,perp} = F^*_{1,perp} * \frac{H^*_{1,N} + \mu * H^*_{1,V}}{H^*_{2,N} + \mu * H^*_{2,V}} \qquad [6.6]$$

The horizontal component F^*_2 is given by:

$$F^*_2 = F^*_{2,perp} * \cos\beta + F^*_{2,paral} * \cos(\frac{\pi}{2} - \beta) \qquad [6.7]$$

In view of eqns. [6.3] and [6.6], equation [6.7] can be written as:

$$F^*_2 = F^*_{1,perp} * \frac{H^*_{1,N} + \mu * H^*_{1,V}}{H^*_{2,N} + \mu * H^*_{2,V}} * (\cos\beta + \mu * \sin\beta) \qquad [6.8]$$

According to equations [6.2] and [3.1]:

$$F^*_{1,perp} * (H^*_{1,N} + \mu * H^*_{1,V}) = F_1 * H_1 \qquad [6.9]$$

$$F^*_{1,perp} = F_1 * \frac{H_1}{H^*_{1,N} + \mu * H^*_{1,V}} \qquad [6.10]$$

In view of eqn. [6.10], equation [6.8] can be written as:

$$F^*_2 = \frac{H_1}{H^*_{2,N} + \mu * H^*_{2,V}} * (\cos\beta + \mu * \sin\beta) * F_1 \qquad [6.11]$$

According to equation [3.9]:

$$F_1 = \frac{F_2}{\cos^2\alpha + \mu * \cos\alpha * \sin\alpha} \qquad [6.12]$$

In the end according to equations [6.11] and [6.12]:

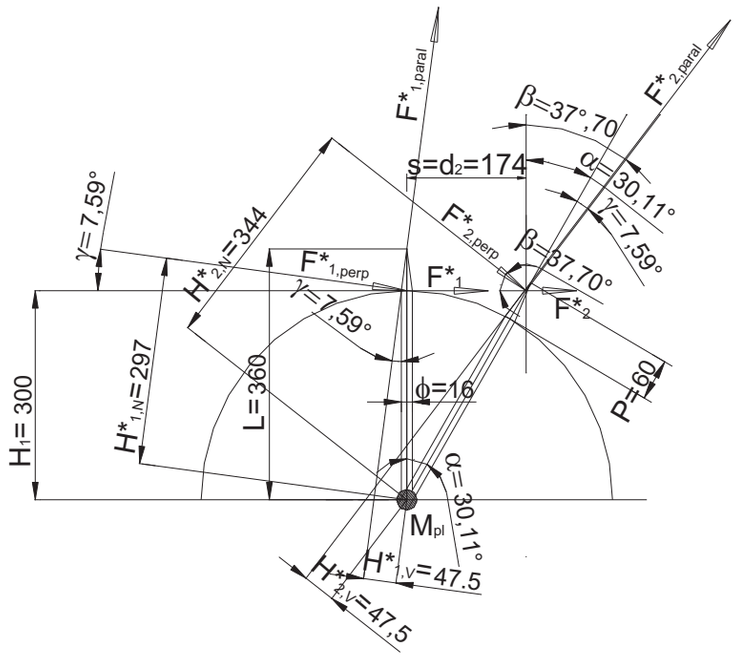

Figure 6.1b - For symbols, see Table 6.1a

$$\frac{F^*_2}{F_2} = \frac{H_1}{H^*_{2,N} + \mu * H^*_{2,V}} * \frac{\cos\beta + \mu * \sin\beta}{\cos^2\alpha + \mu * \cos\alpha * \sin\alpha} \qquad [6.13]$$

Now for the maximum displacement d_2=174mm (maximum displacement of LOKIBASE device at SLC) and zero and non-zero friction a comparison of the horizontal forces at the top of the cylindrical beam damper with conical segment (F^*_2 in the Figure 6.1) and at the top of the cylindrical beam damper (F_2 in the Fi-

Description	Symbol	Unit
Length of the cylindrical beam damper	L	mm
Diameter of the circular cross section of the cylindrical beam damper	ϕ	mm
Length of the conical segment at the top of the cylindrical beam damper	P	mm
Taper angle of the conical segment at the top of the cylindrical beam damper	γ	°
Point of application (=cost.) of the horizontal force F	H_1	mm
Arm of the force perpendicular to the conical segment $F^*_{1,perp}$ for zero displacement	$H^*_{1,N}$	mm
Arm of the force perpendicular to the conical segment $F^*_{2,perp}$ for d_2 displacement	$H^*_{2,N}$	mm
Arm of the force parallel to the conical segment $F^*_{1,paral}$ for zero displacement	$H^*_{1,V}$	mm
Arm of the force parallel to the conical segment $F^*_{2,paral}$ for d2 displacement	$H^*_{2,V}$	mm
Friction coefficient	μ	%
Plastic moment	M_p	Nm
Force for zero displacement $s=0$	F^*_1	N
Force for the maximum displacement $s=d_2$	F^*_2	N
Rotation angle for a s displacement	α	°
Maximum displacement	d_2	mm

Table 6.1a

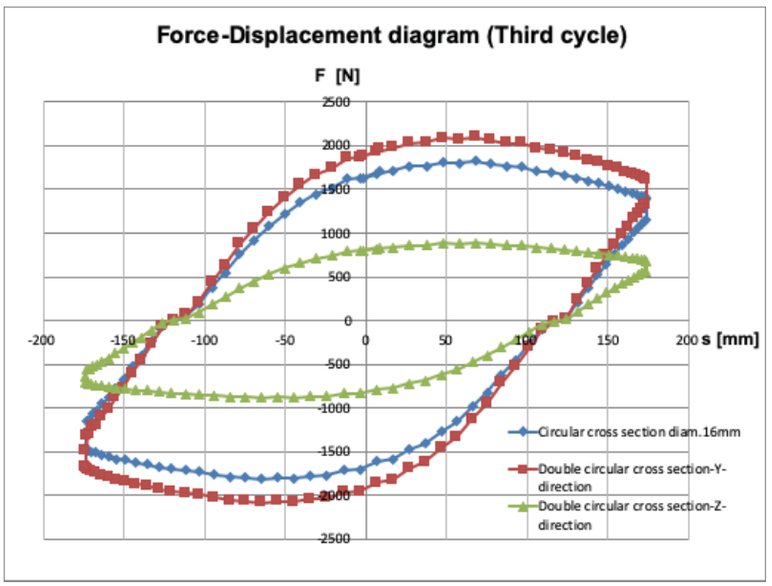

Figure 6.2

gure 3.1) is made:

with zero friction

$$\frac{F_2^*}{F_2} = \frac{H_1}{H_2^*} * \frac{\cos\beta}{\cos^2\alpha} = \frac{300}{344} * \frac{\cos 37.70°}{\cos^2 30.11°} = 0.922 \qquad [6.14]$$

where:

H_1 = 300 mm

H^*_2 = 344 mm

β = 37.70° mm

α = 30.11° mm

with non-zero friction

$$\frac{F_2^*}{F_2} = \frac{H_1}{H^*_{2,N} + \mu * H^*_{2,Y}} * \frac{\cos\beta + \mu * \sin\beta}{\cos^2\alpha + \mu * \cos\alpha * \sin\alpha} = \qquad [6.12]$$

$$= \frac{300}{344 + 0.15 * 47.5} * \frac{\cos 37.70° + 0.15 * \sin 37.70°}{\cos^2 30.11° + 0.15 * \cos 30.11° * \sin 30.11°} = 0.927$$

where:

H_1 = 300 mm

$H^*_{2,N}$ = 344 mm

$H^*_{2,V}$ = 47.5 mm

μ = 15%

β = 37.70°

α = 30.11°

6.3 Optimization analysis of the LOKIBASE cylindrical beam damper. Double- circular cross section at the bottom (in the plastic hinge segment).

In the intended use of LOKIBASE device, it should be remembered the pallet racking systems are special ones because they have different stiffness values in the two principal directions; they are strong in the cross-aisle direction and very weak in the down-aisle direction.

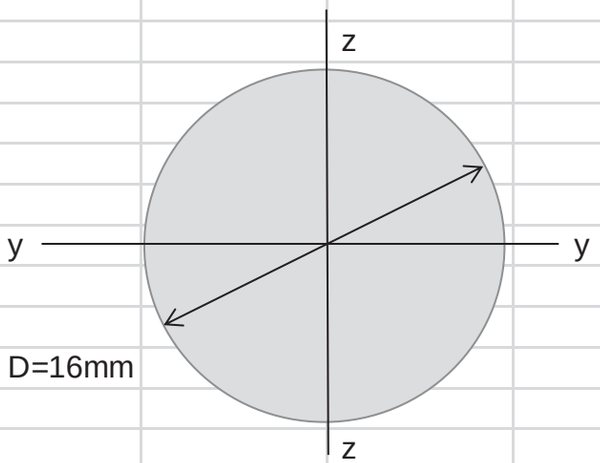

D [mm]=	16	(diameter of the circular cross section)
R [mm]=	8	(radius of the circular cross section)
A [mm^2]=	201	(area of the circular cross section)
y_G [mm]=	3.4	(position of the centre of gravity of the semi-circular cross section along y-axis)
F_G [N]=	101	(force in the centre of gravity of the semi-circular cross section for f_y=1.0 MPa)
M^c_{pl} [Nmm]=	683	(plastic moment of the circular cross section)

Table 6.4

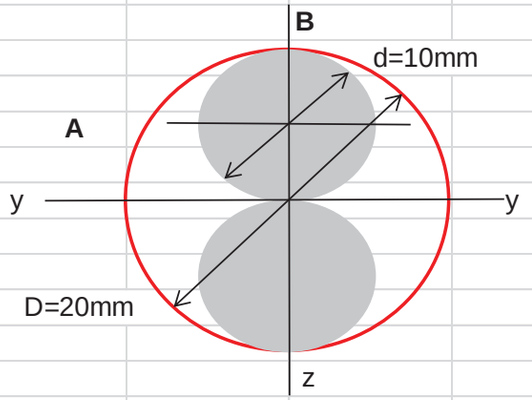

d [mm]=	10	(diameter of one circular cross section in the plastic hinge segment)
r [mm]=	5	(radius of one circular cross section in the plastic hinge segment)
A [mm^2]=	79	(area of one circular cross section in the plastic hinge segment)
y_G [mm]=	2.1	(position of the centre of gravity of one semi-circular cross section in the plastic hinge segment along y-axis)
z_G [mm]=	5.0	(position of the centre of gravity of one circular cross section in the plastic hinge segment along z-axis)
F_G [N]=	39	(force in the centre of gravity of one semi-circular cross section for f_y=1.0 MPa)
$M^{dc}_{pl,yy}$ [Nmm]=	785	(plastic moment of the double circular cross section about y-axis)
$M^{dc}_{pl,zz}$ [Nmm]=	333	(plastic moment of the double circular cross section about z-axis)

Table 6.5

F^{c}_{2} [N]=	1398	(force at the top of the cylindrical beam damper with circular cross section)
$F^{c}_{2,LOKIBASE}$ [N]=	3486	(total force applied to LOKIBASE device)
$E_{d,2\ LOKI}$ [J]=	114	(energy dissipated by two LOKI devices due to friction)
$E^{c}_{d,damper}$ [J]=	781	(energy dissipated by the cylindrical beam damper with circular cross section)
$E^{c}_{d,LOKIBASE}$ [J]=	895	(total energy dissipated by LOKIBASE device)
$\xi^{c}_{e,LOKIBASE}$=	0.235	(LOKIBASE equivalent viscous damping coefficient)

Table 6.7

$F^{dc}_{2,Y}$ [N]=	1608	(force at the top of the cylindrical damper with double circolar cross section at the bottom in Y-direction)
$F^{dc}_{2,Y,LOKIBASE}$ [N]=	3696	(total force applied to LOKIBASE in Y-direction)
$E_{d,2\ LOKI}$ [J]=	114	(energy dissipated by two LOKI devices due to friction)
$E^{dc}_{d,Y,damper}$ [J]=	898	(energy dissipated by the cylindrical damper with double circular cross section at the bottom in Y-direction)
$E^{dc}_{d,Y,LOKIBASE}$ [J]=	1012	(total energy dissipated by LOKIBASE device in Y-direction)
$\xi^{dc}_{e,Y,LOKIBASE}$=	0.25	(LOKIBASE equivalent viscous damping coefficient in Y-direction)

Table 6.8.1

$F^{dc}_{2,Z}$ [N]=	682	(force at the top of the cylindrical damper with double circolar cross section at the bottom in Z-direction)
$F^{dc}_{2,Z,LOKIBASE}$ [N]=	2770	(total force applied to LOKIBASE in Z-direction)
$E_{d,2\ LOKI}$ [J]=	114	(energy dissipated by two LOKI devices due to friction)
$E^{dc}_{d,Z,damper}$ [J]=	381	(energy dissipated by the cylindrical damper with double circular cross section at the bottom in Z-direction)
$E^{dc}_{d,Z,LOKIBASE}$ [J]=	495	(total energy dissipated by LOKIBASE device in Z-direction)
$\xi^{dc}_{e,Z,LOKIBASE}$=	0.16	(LOKIBASE equivalent viscous damping coefficient in Z-direction)

Table 6.8.2

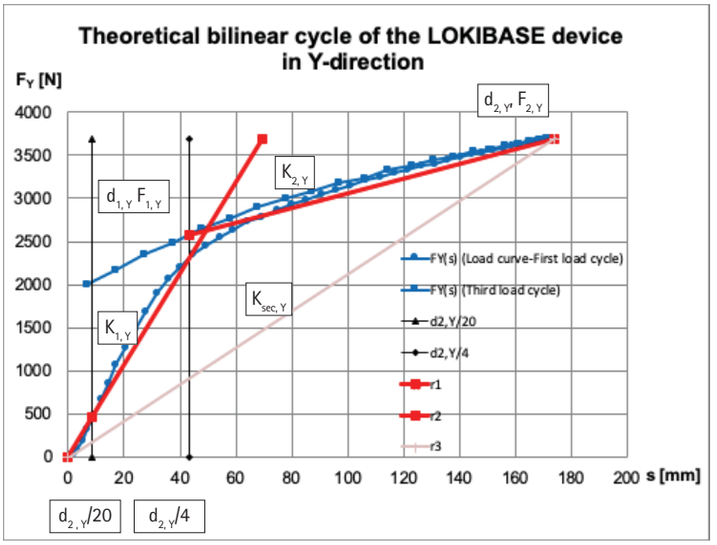

Figure 6.3

As previously mentioned in section 2.1, to get a good control of a pallet racking system under seismic action, in the down-aisle direction is more important to reduce as much as possible the force under earthquake excitation than to reduce the maximum value of the LOKIBASE device displacement using high values of the equivalent viscous damping coefficient. Indeed, in the down-aisle direction the pallet racking systems are self-isolated so that the LOKIBASE device displacement is lower than in the cross-aisle direction.

On the other hand in cross-aisle direction it is necessary to control the maximum value of the LOKIBASE device displacement because in this direction the pallet racking systems are very stiff, all mass of them is on the first mode of vibration, so that about hundred per cent of the displacement is developed by LOKIBASE device.

For pallet racking systems, a rational mitigation in the values of forces and displacements under seismic action is possible by means of a cylindrical beam damper with an optimize shape in the plastic hinge segment.

In this section, the behavior of a cylindrical beam damper with double-circular cross section at the bottom (in the plastic hinge segment) is analyzed and the data about the theoretical bilinear cycle of LOKIBASE device are given.

6.3.1 LOKI device data by test

k [N/mm]=	6.0	(LOKI stiffness)
K [N/mm]=	12.0	(K=2*k=stiffness of two LOKI devices)
$e_{d,LOKI}$ [J]=	57.1	(energy dissipated by LOKI due to friction)
$E_{d,2\ LOKI}$ [J]=	114.1	(energy dissipated by two LOKI devices due to friction)
d_2 [mm]=	174.0	(maximum design displacement of LOKIBASE at the CLS)

Table 6.2

6.3.2 Data of the cylindrical beam damper with circular cross section (diam.16mm) by test

$F^c_{2,damper}$ [N]=	1397.5	(force at d_2)
$E^c_{d,damper}$ [J]=	780.5	(energy dissipated in the third cycle)

Table 6.3

Theoretical bilinear cycle parameters of LOKIBASE device in Y-direction		
Parameter	Value	Note
$d^{dc}_{el,\ Y,\ LOKIBASE}$ [mm]=	8.7	Displacement in the first branch of the load test where the behavior of LOKIBASE device is linear. A value $d_{2,Y}/20$ is taken
$F^{dc}_{el,\ Y,\ LOKIBASE}$ [N]=	460.2	Force for $d^{dc}_{el,LOKIBASE}$ displacement in the first branch of the load test where the behavior of LOKIBASE device is linear
$d^{dc}_{1,\ Y,\ LOKIBASE}$ [mm]=	49.8	Displacement of LOKIBASE device at the intersection point of the r_1 and r_2 straight lines
$F^{dc}_{1,\ Y,\ LOKIBASE}$ [N]=	2637.0	Force on LOKIBASE device at the intersection point of the r_1 and r_2 straight lines
$d^{dc}_{2,Y,LOKIBASE}$ [mm]	173.9	Maximum design displacement of the LOKIBASE device at the Limit state for collapse prevention SLC
$F^{dc}_{2,Y,LOKIBASE}$ [N]=	3694.0	Force on LOKIBASE device for the $d^{dc}_{2,Y,LOKIBASE}$ displacement, in the third cycle of the load test
$K^{dc}_{1,Y,LOKIBASE}$ [N/mm]=	53.0	Elastic stiffness (first branch) of LOKIBASE device
$K^{dc}_{2,,Y,LOKIBASE}$ [N/mm]=	8.5	Post-elastic stiffness (second branch) of LOKIBASE device
$K^{dc}_{sec,Y,LOKIBASE}$ [N/mm]=	21.2	Secant stiffness of LOKIBASE device
μ_{LOKI} [%]=	0.15	Friction coefficient of LOKI devices
$E_{d,2LOKI}$ [J]=	114.1	Energy dissipated by two LOKI devices
$E^{dc}_{d,Y,damper}$ [J]=	898.0	Energy dissipated by the cylindrical beam damper
$E^{dc}_{d,Y,LOKIBASE}$ [J]=	1012.1	Energy dissipated by LOKIBASE device
$\xi^{dc}_{e,Y,LOKIBASE}$=	0.251	LOKIBASE device equivalent viscous damping coefficient
NOTE: (^{dc})Cylindrical beam damper with double-circular cross section at the bottom		

Table 6.9

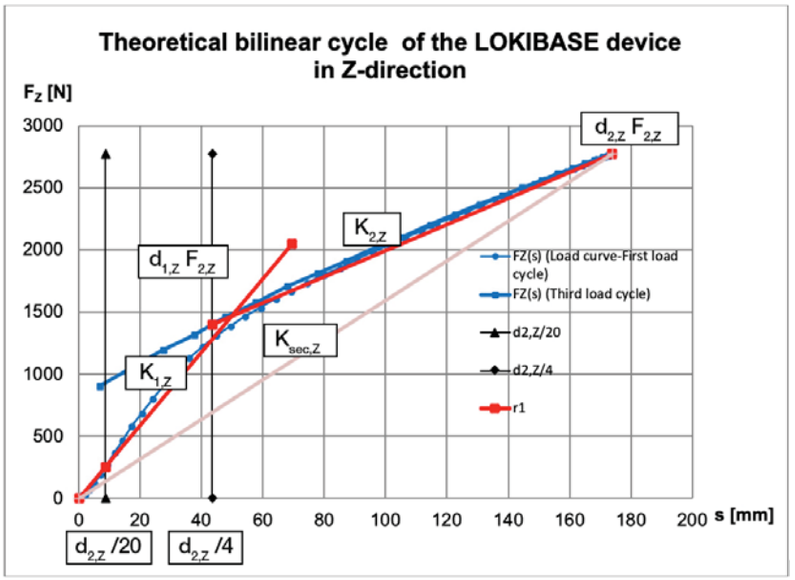

Figure 6.4

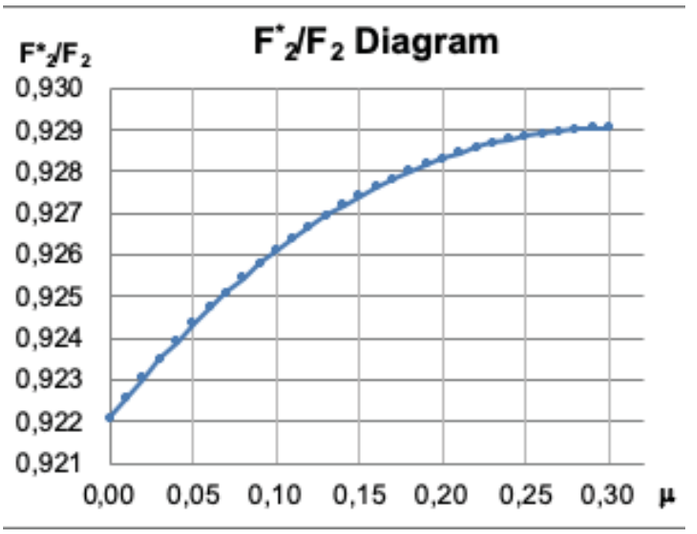

Figure 6.5

6.3.3 Theoretical data of the cylindrical beam damper with circular cross section (diam.16mm)

See Table 6.4

6.3.4 Theoretical data of the cylindrical beam damper with double-circular cross section in the segment at the bottom (plastic hinge segment)

See Table 6.5

6.3.5 Magnification / Reduction factors

$M=M^{dc}_{pl,yy}/M^{c}_{pl}$	1.15	(magnification factor M about y-axis)
$R=M^{dc}_{pl,zz}/M^{c}_{pl}$	0.49	(reduction factor R about z-axis)

Table 6.6

6.3.6 Energy dissipated in the third cycle by the cylindrical beam dampers with circular and double-circular cross section in the segment at the bottom in Y and Z direction

See Figure 6.2

Theoretical bilinear cycle parameters of LOKIBASE device in Z-direction		
Parameter	Value	Note
$d^{dc}_{el,\,Z,\,LOKIBASE}$ [mm]=	8.7	Displacement in the first branch of the load test where the behavior of LOKIBASE device is linear. A value $d_{2,Z}/20$ is taken
$F^{dc}_{el,\,Z,\,LOKIBASE}$ [N]=	255.9	Force for $d^{dc}_{el,LOKIBASE}$ displacement in the first branch of the load test where the behavior of LOKIBASE device is linear
$d^{dc}_{1,\,Z,\,LOKIBASE}$ [mm]=	49.8	Displacement of LOKIBASE device at the intersection point of the r_1 and r_2 straight lines
$F^{dc}_{1,\,Z,\,LOKIBASE}$ [N]=	1466.3	Force on LOKIBASE device at the intersection point of the r_1 and r_2 straight lines
$d^{dc}_{2,Z,LOKIBASE}$ [mm]	173.9	Maximum design displacement of the LOKIBASE device at the Limit state for collapse prevention SLC
$F^{dc}_{2,Z,LOKIBASE}$ [N]=	2771.7	Force on LOKIBASE device for the $d^{dc}_{2,Z,LOKIBASE}$ displacement, in the third cycle of the load test
$K^{dc}_{1,Z,LOKIBASE}$ [N/mm]=	29.5	Elastic stiffness (first branch) of LOKIBASE device
$K^{dc}_{2,,Z,LOKIBASE}$ [N/mm]=	10.5	Post-elastic stiffness (second branch) of LOKIBASE device
$K^{dc}_{sec,Z,LOKIBASE}$ [N/mm]=	15.9	Secant stiffness of LOKIBASE device
μ_{LOKI} [%]=	0.15	Friction coefficient of LOKI devices
$E_{d,2LOKI}$ [J]=	114.1	Energy dissipated by two LOKI devices
$E^{dc}_{d,Z,damper}$ [J]=	381.1	Energy dissipated by the cylindrical beam damper
$E^{dc}_{d,Z,LOKIBASE}$ [J]=	495.3	Energy dissipated by LOKIBASE device
$\xi^{dc}_{e,Z,LOKIBASE}$=	0.164	LOKIBASE device equivalent viscous damping coefficient
NOTE: (dc)Cylindrical beam damper with double-circular cross section at the bottom		

Table 6.10

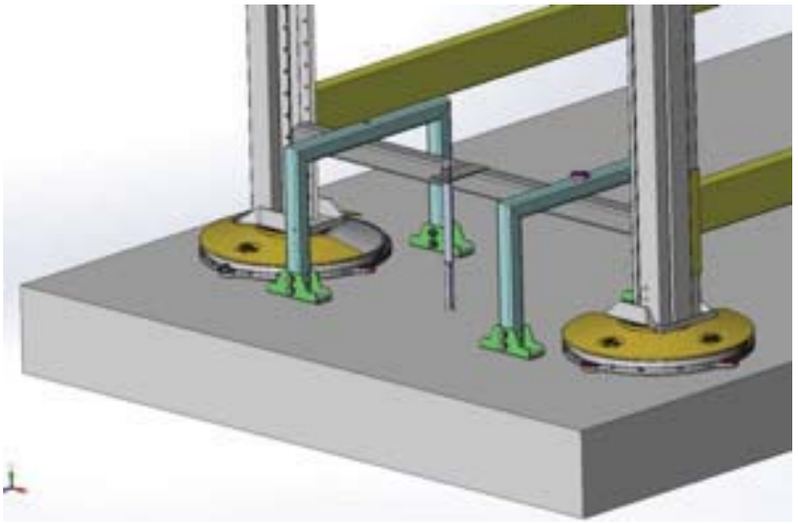

Figure 7.1.1 – View of the equipment

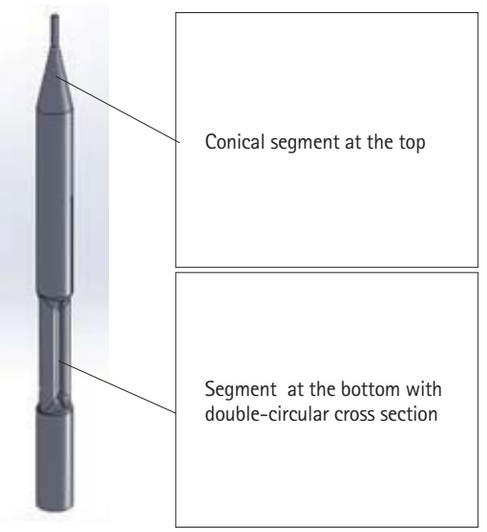

Figure 7.1.2 – Optimize cylindrical beam damper

6.3.7 Force applied to and energy dissipated by the LOKIBASE device (cylindrical beam damper with circular cross section diam.16mm)

See Table 6.7

6.3.8 Force applied to and energy dissipated by the optimized LOKIBASE device (cylindrical beam damper with double-circular cross section inscribed in a circle of diam. 20mm in the segment at the bottom)

See Tables 6.8.1 and 6.8.2.

Now, for the maximum displacement d_2 and two LOKI devices with a k value of 6 N/mm, a comparison of the horizontal force acting in Z-direction (down-aisle direction, the weakest) on the LOKIBASE device with optimized cylindrical beam damper ($F^{dc}_{2,Z,LOKIBASE}$ in the Table 6.8.2) and the horizontal force acting in the same direction on the LOKIBASE device with cylindrical beam damper ($F^{c}_{2,LOKIBASE}$ in the Table 6.7) is made.

$$\frac{F^{dc}_{2,Z,LOKIBASE}}{F^{c}_{2,LOKIBASE}} = \frac{2770}{3486} = 0.79 \qquad [6.16]$$

6.3.9 Theoretical bilinear cycles of the LOKIBASE device

In Figure 6.3, the theoretical elastic behavior of the LOKIBASE device in Y-direction is shown.

Note: In the Figure 6.3 (^{dc}) superscript and ($_{LOKIBASE}$) subscript are not reported.

In Table 6.9 the data of the theoretical bilinear cycle of the LOKIBASE device in Y-direction are summarize.

In Figure 6.4, the theoretical elastic behavior of the LOKIBASE device in Z-direction is shown.

Note: In Figure 6.4 $^{(dc)}$ superscript and (LOKIBASE) subscript are not reported.

In the following Table 6.10 the data of the theoretical bilinear cycle of the LOKIBASE device in Z-direction are summarize.

$F^{dc*}_{2,Y}$ [N]=	1490	(force at the top of the cylindrical beam damper with double circolar cross section at the bottom and engaged conical segment in Y-direction)
$F^{dc*}_{2,Y,LOKIBASE}$ [N]=	3230	(total force applied to LOKIBASE in Y-direction)
$E_{d,2\ LOKI}$ [J]=	114	(energy dissipated by two LOKI devices due to friction)
$E^{dc*}_{d,Y,damper}$ [J]=	898	(energy dissipated by the cylindrical beam damper with double circular cross section at the bottom and engaged conical segment in Y-direction)
$E^{dc*}_{d,Y,LOKIBASE}$ [J]=	1012	(total energy dissipated by LOKIBASE device in Y-direction)
$\xi^{dc*}_{e,Y,LOKIBASE}$=	0.29	(LOKIBASE equivalent viscous damping coefficient in Y-direction)

Table 7.3.1

$F^{dc*}_{2,Z}$ [N]=	633	(force at the top of the cylindrical beam damper with double circolar cross section at the bottom and engaged conical segment in Z-direction)
$F^{dc*}_{2,Z,LOKIBASE}$ [N]=	2373	(total force applied to LOKIBASE in Z-direction)
$E_{d,2\ LOKI}$ [J]=	114	(energy dissipated by two LOKI devices due to friction)
$E^{dc*}_{d,Z,damper}$ [J]=	381	(energy dissipated by the cylindrical beam damper with double circular cross section at the bottom and engaged conical segment in Z-direction)
$E^{dc*}_{d,Z,LOKIBASE}$ [J]=	495	(total energy dissipated by LOKIBASE device in Z-direction)
$\xi^{dc*}_{e,Z,LOKIBASE}$=	0.19	(LOKIBASE equivalent viscous damping coefficient in Z-direction)

Table 7.3.2

6.4 Conclusions

Eqn. [6.14] and eqn. [6.15] in section 6.2 show that engaging a conical segment the percentage reduction in the value of the horizontal force F_2 (eqn. [3.10]) only slightly depend on the friction coefficient values. In the range 0-15% of the friction values, the shape optimization of the segment at the top of the cylindrical beam damper allows a reduction of about 7.5% in the value of the horizontal force F_2 (Figure 6.5).

In section 6.3 is shown that, in the down-aisle direction (Z-direction) the shape optimization of the segment at the bottom of the cylindrical beam damper allows:

a) to reduce the horizontal force at the top of the cylindrical beam damper from F^c_2=1398 N to $F^{dc}_{2,Z}$=682 N. The ratio of the $F^{dc}_{2,Z}$ (force which engages the cylindrical beam damper with double-circular cross section) to the F^c_2,(force which engages the cylindrical beam damper with circular cross section) is 0.49 (a reduction of 51% in the value of F^c_2);

b) to reduce the horizontal force on the LOKIBASE device from $F^c_{2,LOKIBASE}$ = 3486 N to $F^{dc}_{2,Z,LOKIBASE}$ =2770 N when the elastic behavior of the two LOKI devices is characterized by a k value of 6 N/mm. For this k value the ratio of the $F^{dc}_{2,Z,LOKIBASE}$ (see Table 6.8.2) to the $F^c_{2,LOKIBASE}$ (see Table 6.7) is 0.79 (a reduction of 20.5% in the value of $F^c_{2,LOKIBASE}$);

In the same section, is shown that, in the cross-aisle direction (Y-direction) the shape optimization of the segment at the bottom of the cylindrical beam damper allows to rise the equivalent viscous damping coefficient $\xi_{e,Y,LOKIBASE}$ from 23.5% (see Table 6.7) to 25% (see Table 6.8.1). In the cross-aisle direction the LOKIBASE device displacement value is reduced about of 2.5%.

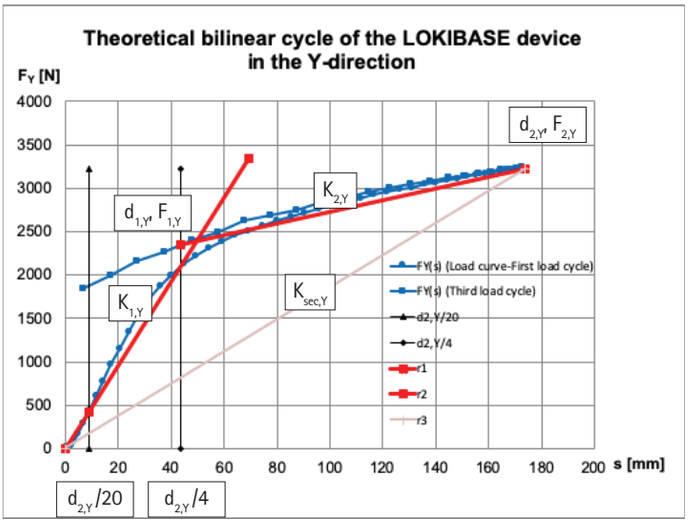

Figure 7.2

7 OPTIMIZATION ANALYSIS OF THE LOKIBASE DEVICE

7.1 Introduction

The theoretical optimization analysis shown below aims to optimize the behavior of LOKIBASE device in order to:

- reduce the force under earthquake excitation in the down-aisle direction (Z-direction);
- control the maximum value of the displacement in the cross-aisle direction (Y-direction).

Theoretical bilinear cycle parameters of LOKIBASE device in Y-direction		
Parameter	**Value**	**Note**
$d^{dc*}_{el,Y,LOKIBASE}$ [mm]=	8.7	Displacement in the first branch of the load test where the behavior of LOKIBASE device is linear. A value $d_{2,Y}/20$ is taken
$F^{dc*}_{el,Y,LOKIBASE}$ [N]=	416.9	Force for $d^{dc*}_{el,LOKIBASE}$ displacement in the first branch of the load test where the behavior of LOKIBASE device is linear
$d^{dc*}_{1,Y,LOKIBASE}$ [mm]=	49.8	Displacement of LOKIBASE device at the intersection point of the r_1 and r_2 straight lines
$F^{dc*}_{1,Y,LOKIBASE}$ [N]=	2388.6	Force on LOKIBASE device at the intersection point of the r_1 and r_2 straight lines
$d^{dc*}_{2,Z,LOKIBASE}$ [mm]	173.9	Maximum design displacement of the LOKIBASE device at the Limit state for collapse prevention SLC
$F^{dc*}_{2,Z,LOKIBASE}$ [N]=	3228.9	Force on LOKIBASE device for the $d^{dc*}_{2,Y,LOKIBASE}$ displacement, in the third cycle of the load test
$K^{dc*}_{1,Y,LOKIBASE}$ [N/mm]=	48.0	Elastic stiffness (first branch) of LOKIBASE device
$K^{dc*}_{2,Y,LOKIBASE}$ [N/mm]=	6.8	Post-elastic stiffness (second branch) of LOKIBASE device
$K^{dc*}_{sec,Y,LOKIBASE}$ [N/mm]=	18.6	Secant stiffness of LOKIBASE device
μ_{LOKI} [%]=	0.15	Friction coefficient of LOKI devices
$E_{d,2LOKI}$ [J]=	114.1	Energy dissipated by two LOKI devices
$E^{dc*}_{d,Y,damper}$ [J]=	898.0	Energy dissipated by the cylindrical beam damper
$E^{dc*}_{d,Y,LOKIBASE}$ [J]=	1012.1	Energy dissipated by LOKIBASE device
$\xi^{dc*}_{e,Y,LOKIBASE}$=	0.287	LOKIBASE device equivalent viscous damping coefficient
NOTE: $^{(dc*)}$Cylindrical beam damper with double-circular cross section at the bottom and conical segment at the top		

Table 7.4

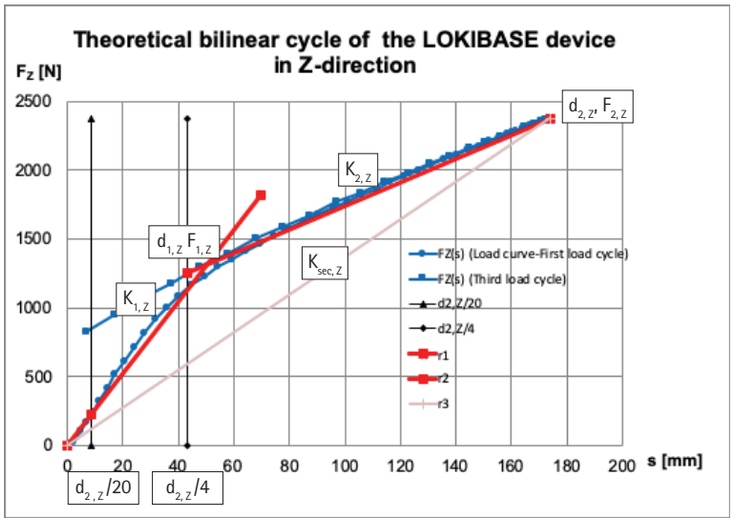

Figure 7.3

For the maximum displacement d_2, a comparison of the horizontal force acting in Z-direction (down-aisle direction, the weakest) on the optimized LOKIBASE device ($F^{dc*}_{2,Z,LOKIBASE}$ in the Table 7.3.2) and the horizontal force acting in the same direction on the LOKIBASE device with cylindrical beam damper ($F^{c}_{2,LOKIBASE}$ in the Table 6.7) is made.

The data about the theoretical bilinear cycle of the optimized LOKIBASE device are given.

In the Figures 7.1.1-7.1.2 the analyzed equipment is shown.

7.2 Optimization analysis of the LOKIBASE device

The theoretical optimization analysis takes account of:

- LOKI device stiffness k=5 N/mm;
- segment at the bottom of the LOKIBASE cylindrical beam damper with double- circular cross section (in the plastic hinge section);
- conical segment at the top of the LOKIBASE cylindrical beam damper with non-zero friction.

7.2.1 LOKI device data by test

Table 7.1

k [N/mm]=	5.0	(LOKI stiffness)
K [N/mm]=	10.0	(K=2*k=stiffness of two LOKI devices)
$e_{d,LOKI}$ [J]=	57.1	(energy dissipated by LOKI due to friction)
$E_{d,2\ LOKI}$ [J]=	114.1	(energy dissipated by two LOKI devices due to friction)
d_2 [mm]=	174.0	(maximum design displacement of LOKIBASE at the CLS)

7.2.2 Data of the cylindrical beam damper with circular cross section (diam.16mm) and engaged conical segment by test

Table 7.2

$F^{c}_{2,damper}$ [N]=	1397.5	(force at the maximum displacement d_2 when the engaged segment is cylindical)
$r_{conical}=F^{*}_{2}/F_2$	0.927	(theoretical coefficient for engaged conical segment - see [7.25])
$F^{c*}_{2,damper}$ [N]=	1295.5	(force at the maximum displacement d_2 when the engaged segment is conical)
$E^{c*}_{d,damper}$ [J]=	780.5	(energy dissipated in the third cycle when the engaged segment is conical)

7.2.3 Theoretical data of the cylindrical beam damper with circular cross section (diam.16mm)

See Table 6.3.

Theoretical bilinear cycle parameters of LOKIBASE device in Z-direction		
Parameter	Value	Note
$d^{dc*}_{el,Z,LOKIBASE}$ [mm]=	8.7	Displacement in the first branch of the load test where the behavior of LOKIBASE device is linear. A value $d_{2,Z}/20$ is taken
$F^{dc*}_{el,Z,LOKIBASE}$ [N]=	227.5	Force for $d^{dc*}_{el,Z,LOKIBASE}$ displacement in the first branch of the load test where the behavior of LOKIBASE device is linear
$d^{dc*}_{1,Z,LOKIBASE}$ [mm]=	49.8	Displacement of LOKIBASE device at the intersection point of the r_1 and r_2 straight lines
$F^{dc*}_{1,Z,LOKIBASE}$ [N]=	1303.3	Force on LOKIBASE device at the intersection point of the r_1 and r_2 straight lines
$d^{dc*}_{2,Z,LOKIBASE}$ [mm]	173.9	Maximum design displacement of the LOKIBASE device at the Limit state for collapse prevention SLC
$F^{dc*}_{2,Z,LOKIBASE}$ [N]=	2373.9	Force on LOKIBASE device for the $d^{dc*}_{2,Z,LOKIBASE}$ displacement, in the third cycle of the load test
$K^{dc*}_{1,Z,LOKIBASE}$ [N/mm]=	26.2	Elastic stiffness (first branch) of LOKIBASE device
$K^{dc*}_{2,Z,LOKIBASE}$ [N/mm]=	8.6	Post-elastic stiffness (second branch) of LOKIBASE device
$K^{dc*}_{sec,Z,LOKIBASE}$ [N/mm]=	13.7	Secant stiffness of LOKIBASE device
μ_{LOKI} [%]=	0.15	Friction coefficient of LOKI devices
$E_{d,2LOKI}$ [J]=	114.1	Energy dissipated by two LOKI devices
$E^{dc*}_{d,Z,damper}$ [J]=	381.1	Energy dissipated by the cylindrical beam damper
$E^{dc*}_{d,Z,LOKIBASE}$ [J]=	495.3	Energy dissipated by LOKIBASE device
$\xi^{dc*}_{e,Z,LOKIBASE}$=	0.191	LOKIBASE device equivalent viscous damping coefficient
NOTE: $^{(dc*)}$Cylindrical beam damper with double-circular cross section at the bottom and conical segment at the top		

Table 7.5

Code	Force acting on two LOKI devices at d_2=174 mm		Force acting on LOKIBASE cylindrical beam damper in Z-direction at d_2=174 mm			Total force acting on LOKIBASE device in Z-direction at d_2=174 mm	Percent reduction (with reference to Code A)	Percent reduction (with reference to Code B)
	N		N			N	%	%
	Standard LOKI	Optimized LOKI	Standard beam damper		Optimized beam damper			
	LOKI device stiffness k=6 N/mm	LOKI device stiffness k=5 N/mm	Without second order effects	With second order effects	With second order effects			
A	2088		1716			3804		
B	2088			1399		3487		
C		1740			633	**2373**	**37.5**	**32.0**
LOKIBASE DEVICE CONFIGURATIONS								
Note	Code A	k=6 N/mm; cylindrical beam damper with circular cross section and without second order effects (Theoretical configuration only)						
	Code B	k=6 N/mm; cylindrical beam damper with circular cross section and with second order effects (Standard configuration – chapter 5)						
	Code C	k=5 N/mm; optimize cylindrical beam damper with second order effects (Optimized configuration – chapter 7)						

Table 7.6

7.2.4 Theoretical data of the cylindrical beam damper with double-circular cross section in the segment at the bottom (plastic hinge segment)

See Table 6.4.

7.2.5 Magnification / Reduction factors

See Table 6.5.

7.2.6 Energy dissipated in the third cycle by the cylindrical beam dampers with circular and double-circular cross section in the segment at the bottom in Y and Z direction

See Figure 6.1.

7.2.7 Force applied to and energy dissipated by the optimized LOKIBASE device (cylindrical beam damper with double-circular cross section inscribed in a circle of diam. 20mm in the segment at the bottom and engaged conical segment at the top)

See Tables 7.3.1 and 7.3.2.

Now, for the maximum displacement d_2 and two LOKI devices with a k value of 5 N/mm, a comparison of the horizontal force acting in Z-direction (down-aisle direction, the weakest) on the optimized LOKIBASE device ($F^{dc*}_{2,Z,LOKIBASE}$ in the Table 7.3.2) and the horizontal force acting in the same direction on the LOKIBASE device with cylindrical beam damper ($F^{c}_{2,LOKIBASE}$ in the Table 6.7) is made.

$$\frac{F^{dc*}_{2,Z,LOKIBASE}}{F^{c}_{2,LOKIBASE}} = \frac{2373}{3486} = 0.68 \qquad [7.1]$$

7.2.8 Theoretical bilinear cycles of the LOKIBASE device

In the Figure 7.2, the theoretical elastic behavior of the LOKIBASE device in Y-direction is shown.

Note: In the Figure 7.2 (^{dc*}) superscript and ($_{LOKIBASE}$) subscript are not reported.

In the Table 7.4 the data of the theoretical bilinear cycle of the optimized LOKIBASE device in Y-direction are summarize.

In Figure 7.3, the theoretical elastic behavior of the LOKIBASE device in Z-direction is shown.

Note: In the Figure 7.3 (^{dc*}) superscript and ($_{LOKIBASE}$) subscript are not reported.

In Table 7.5 the data of the theoretical bilinear cycle of the optimized LOKIBASE device in Z-direction are summarize.

7.3 Conclusions

In section 7.2 is shown that, in the down-aisle direction (Z-direction) a reduction in the stiffness value of the LOKI devices (from k=6 N/mm to k=5 N/mm) and the shape optimization of the segments at the top and at the bottom of the cylindrical beam damper allow to reduce the horizontal force on the LOKIBASE device from $F^{c}_{2,LOKIBASE}$=3486 N (LOKI devices with k=6 N/mm and LOKIBASE beam damper with circular cross section diam.16 mm – Table 6.7) to $F^{dc*}_{2,Z,LOKIBASE}$ =2373 N (optimized LOKIBASE device – Table 7.3.2). The ratio of the $F^{dc*}_{2,Z,LOKIBASE}$ to the $F^{c}_{2,LOKIBASE}$ is 0.68 (a reduction of 32% in the value of the $F^{c}_{2,LOKIBASE}$).

In the same section, is shown that, in the cross-aisle direction (Y-direction) a reduction in the stiffness value of the LOKI devices (from k=6 N/mm to k=5 N/mm) and a shape optimization of the segments at the top and at the bottom of the cylindrical

beam damper allow to rise the equivalent viscous damping coefficient $\xi_{e,Y,LOKIBASE}$ from 23.5% (LOKI devices with k=6 N/mm and LOKIBASE cylindrical beam damper with circular cross section diam.16 mm – Table 6.7) to 29% (optimized LOKIBASE device – Table 7.3.1). In the cross-aisle direction the LOKIBASE device displacement value is reduced about of 8.0%.

In the Table 7.6 the percent reductions in the horizontal force acting on the optimized LOKIBASE device (code C) with reference to the standard configuration (code B) and to the theoretical configuration (code A) are given.

Manufacturer:

Girardini S.r.l. - Via Fabbrica 90/92 – 38079 Tione di Trento (TN)
tel.0465/339111 – mail: girardini@girardini.it – website: www.girardini.it

8 LOKIBASE TESTING (PICTURES)

Picture 8.1 – Cyclic flexural testing on LOKI devices by ALGA. Picture Picture 8.2 – Shaking table testing on LOKI devices by National Technical University of Atene Picture 8.3 – Shaking table testing on LOKIBASE devices by Girardini Laboratory. Picture 8.4 - Shaking table testing on Pallet Racking System (with LOKIBASE devices) by Girardini Laboratory. Picture 8Picture 8.10 – Cylindrical beam damper with double- circular cross section.

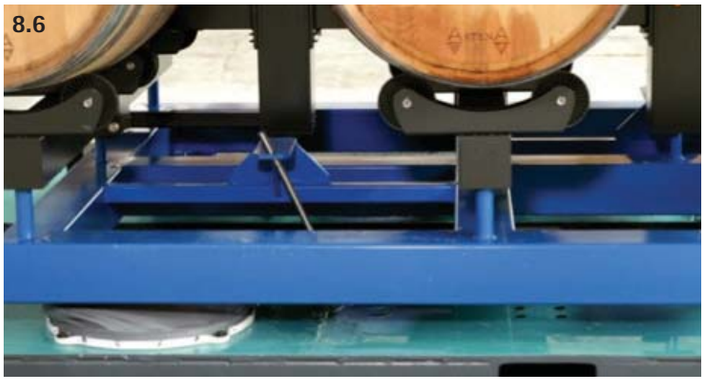

Picture 8.6 - Shaking table testing on Wine Barrel Rack (with LOKIBASE devices) by Girardini Laboratory. Picture 8.7 - Shaking table testing on Wine Barrel Rack (without LOKIBASE devices) by Girardini Laboratory. Picture 8.8 -Shaking table testing on Pallet Racking System (without LOKIBASE devices)by Girardini Laboratory. Picture 8.9 –LOKI device. Picture 8.10 – Cylindrical beam damper with double- circular cross section.

RIFERIMENTI BIBLIOGRAFICI

[1] Camporesi G., Ceroni P. (2014). Relazione di verifica delle performance e specifiche del dispositivo antisismico per scaffalature tipo LOKI;

[2] Castiglioni C, Quaglini V. (2010). Linea Guida per il rilascio dell'Attestato di Qualificazione per Isolatori Antisismici per Scaffalature Industriali BASE GFMI;

[3] Castiglioni C, Quaglini V. (2010). Rapporto di Valutazione per Isolatori Antisismici per Scaffalature Industriali BASE GFMI;

[4] NTC (2018). Norme tecniche per le costruzioni, DM 17 gennaio 2018, published in the Gazzetta Ufficiale n.42 of 20 February 2018 – Suppl. Ordinario n.8;

[5] Zandonini R., Molinari M (2015). Certificato di prova n°LPMS 045/2015 – Prova di barre d'acciaio inox diam.16mm a trazione, a flessione monotona e ciclica a frequenza 0.5 Hz in un vincolo metallico e inghisate con resina in calcestruzzo

[6] NTC (2018). Norme tecniche per le costruzioni, DM 17 gennaio 2018, published in the Gazzetta Ufficiale n.42 of 20 February 2018 – Suppl. Ordinario n.8.